Options for Daytime Monitoring of Atmospheric Visibility in Optical Communications

D. Erickson and K. Cowles
Communications Systems Research Section

Techniques for daytime detection of atmospheric transmission and cloud cover to determine the capabilities of future deep-space optical communications links are considered. A modification of the planned nighttime photometry program will provide the best data while minimizing the need for further equipment. Greater degrees of modification will provide increased detection capabilities. Future testing of the equipment will better define the improvement offered by each level of modification. Daytime photometry is favored at certain wavelengths because of higher transmission and lower background noise, thus giving an increased signal-to-noise ratio. A literature search has provided a list of stars brighter than second magnitude at these wavelengths.

I. Introduction

The Atmospheric Visibility Monitoring (AVM) program will monitor the presence and correlation of cloud cover and transmission through the atmosphere at certain laser wavelengths to determine the feasibility of accommodating a cluster of ground-based optical communications transceivers. The sky must be continuously monitored, 24 hours a day, to detect clouds and transmission at varying zenith angles. At night, starlight will be detected using differential stellar photometry from three automatic photoelectric telescopes (APTs) on mountains in the southwestern United States. Equipment for nighttime photometry has already been purchased. During the day, detection of clouds and measurement of atmospheric transmission using stellar photometry are more challenging because of the background noise caused by scattered sunlight. Several different options were considered for use in monitoring the atmosphere during the day.

II. Criteria

The criteria which need to be met by a daytime AVM detection scheme are as follows:

(1) Detect the presence of clouds as a percentage of sky cover

(2) Monitor the entire sky, especially near the ecliptic, throughout the day

(3) Measure atmospheric transmission at varying zenith angles

(4) Maintain autonomous operation

(5) Keep additional equipment costs to a minimum

(6) Require minimal maintenance (a system could operate for periods of 2–3 months without trained personnel traveling to the site for maintenance)

(7) Do not point the telescope at the sun because of potential damage

III. Candidate Monitoring Techniques

Several monitoring options were considered, including

(1) Pyroheliometer mounted on a solar tracker

(2) A pair of pyranometers, one with a shadow band

(3) Polaris monitor

(4) All-sky camera

(5) Blue-sky monitor

(6) Modified daytime stellar photometry

A. Pyroheliometer

This technique uses a simple solar radiation sensor mounted on a solar tracker. The sensor measures normally incident solar radiation [1]. The advantages of this technique are that it is capable of measuring atmospheric transmission as a function of solar intensity, is simple, needs very little direct maintenance, and eliminates the need to use the telescope when the sun is up.

However, several disadvantages arise from the fact that only normally incident radiation is measured. Cloud and transmission information would only be measured from a direct line to the sun. Broadband transmission would be measured instead of transmission at specific wavelengths. Cloud cover would not be measured as a percentage of the whole sky, but only if a cloud was between the sun and the detector. Changing solar zenith angle and solar magnitude would complicate the data processing and make the results less well-defined. Also, new equipment would have to be purchased. The added hardware expense would be approximately $10,000 per station.

B. Pyranometers

This is also a passive solar radiation system. This technique uses two all-sky, solar radiation sensors [1]. One sensor is exposed to the whole sky. The other sensor has a shadow band that blocks the sun's path. By comparing the measurements of the two pyranometers, direct solar radiation can be calculated.

This system is simpler than the pyroheliometer because it has no moving parts. The cost is approximately the same. It has basically the same advantages and disadvantages as a pyroheliometer, but would make it slightly easier to process the data. This is because changes in solar magnitude will cancel out.

C. Polaris Monitor

A Polaris monitor uses a smaller telescope system to monitor the star Polaris throughout the day. This has the advantage of being simple. Polaris, also known as the North Star, moves approximately 90 arc minutes during a 24-hour period. The Polaris monitor also has the advantage of obtaining atmospheric transmission data. This technique's major disadvantage is that it is not an all-sky technique. In fact, it looks at the sky as far away from the ecliptic as possible. It would also require purchasing a second telescope and controller for each site at a cost of approximately $10,000 apiece.

D. All-sky Camera

Two institutions are using a camera with a wide-angle lens (170-deg FOV), to obtain cloud-cover information. One institution uses film and the other uses a charge-coupled device (CCD) camera [2,3]. Of the six options studied, these cameras have the best all-sky capabilities. However, they both have the disadvantage of being difficult to run remotely for long periods of time. The film camera must have its film changed regularly. The CCD system gathers approximately 150 megabytes of data in a 12-hour day. Transferring this data over a modem would be time- and cost-prohibitive. Storage of the data for long periods would also be very difficult. Another major disadvantage of this technique is that it would not gather any atmospheric transmittance data. It can only describe where the clouds are at any given time. The CCD systems cost approximately $25,000 each.

E. Blue-sky Monitor

By using the photometer on the APT, the sky could be monitored for clouds. This idea calls for the telescope to sweep periodically across the daytime sky and take photometric measurements using red and blue filters. The data received would be nearly identical to the all-sky camera data. The hardware cost would be minimal. However, developing the data-reduction algorithm and filter design might be difficult.[1] Like the all-sky camera, this scheme would not obtain any atmospheric transmittance data. A worrisome aspect of this technique is the potential damage to the telescope and photometer if the telescope sweeps across the sun. This problem should be solved if the control software is written with enough care.

F. Modified Daytime Stellar Photometry

Using the same methods day and night would be highly convenient when processing and comparing data. Just as it

---

[1] According to R. W. Johnson, manager of the CCD All-sky Camera project at the Scripps Institution in San Diego, California, the blue-red filter techniques they use were difficult to develop.

would at night, photometry used during the day will yield the most interesting transmission and cloud cover data. Performing standard UBV-differential photometry in the daytime would be difficult with the present system. UBV photometry measures starlight at three spectral bands: ultraviolet or U (centers at 350 nm), blue or B (Centers at 435 nm), and visible or V (Centers at 550 nm). The background noise caused by solar irradiance is too high at these wavelengths to perform daytime photometry. Two ways in which daytime photometry could be modified using the APT are selecting the correct band-pass filters and optically modifying the photometer.

Five issues need to be considered for selecting the correct band-pass filters for use during the day. They are as follows:

1. Photometric Standards. Doing stellar photometry would be simplified and more accurate if the system monitors wavelengths that have well-documented intensities. Some possible photometric standards that are within the range of the existing photometer are ultraviolet/blue/visible/red/infrared (UBVRI) filters, as established by Johnson [4, 5]. The UBVRI bands center near 350 nm, 435 nm, 555 nm, 700 nm, and 860 nm, respectively. They have bandwidths that range from 90–140 nm. The Wing MA, MB, and MI filters, a fairly new standard, center at 712 nm, 754 nm, and 1025 nm, respectively [5]. Their bandwidths are 10–40 nm.

2. Photometer Range. The photometer uses a Hamamatsu silicon PIN-photodiode with a usable spectral range of 320–1050 nm [5].

3. Solar Radiation. Solar irradiance peaks around 500 nm and then decreases sharply with increasing wavelength. Figure 1 shows that at 1000 nm the solar irradiance is at about one-third of the irradiance at 500 nm. The signal-to-noise ratio will improve at longer wavelengths.

4. Atmospheric Absorption. Certain wavelengths will not transmit as well through the atmosphere because of molecular absorption bands; however, in general the atmospheric transmission increases with wavelength, as shown in Fig. 2.

5. Communication Wavelengths. The most likely wavelengths to be used for future deep-space optical communication links are 532 nm, 810 nm, and 1064 nm.

After considering these five variables, it has been determined that the best filters to use for daytime photometry in the AVM project are the MI filter at 1025 nm and the I filter at 860 nm.

Daytime photometry can also be optimized by optically modifying the photometer. Decreasing the photometer's dia-

phragm diameter by one-half can improve the signal-to-noise ratio by a factor of four. The standard photometer has a diaphragm diameter of 1 mm, producing a 90-arc-second field of view. A simple Barlow lens mounted in the telescope's optical path, normally used as an image magnifier, will decrease the field of view of the telescope by the power of the lens. This can also increase the signal-to-noise ratio. Making these modifications will enable the detection of stars 1.5 to 3 magnitudes dimmer than possible with an unmodified APT. This will more than double the number of stars that can be observed.

Decreasing the diaphragm and using a Barlow lens does create some difficulties. The APTs search and centering function will be slowed down substantially since the field of view is decreased. This slowdown will decrease the number of stars the system can monitor in a given period of time. In the day, this may not present a problem because of the limited number of bright stars. At night, however, the longer search and centering function will greatly limit the quantity of stars observed. Adding an instrument selector with day and night photometers will increase the day performance without limiting the night program. An instrument selector and a second photometer will cost approximately $7,000 for each system.

A dew cap will be used at night to prevent dewing problems. During the day the dew cap will act as a simple sunshade, preventing some scattered sunlight from entering the aperture of the telescope.

Modified daytime stellar photometry meets all the criteria. It has the advantage of requiring minor equipment changes. It will provide daytime data in the same form as nighttime data, thus simplifying data analysis.

There is the possibility of damage to the telescope and photometer if the telescope sweeps across the sun. The control software can be written to avoid this problem. Some modifications will slow down the search and centering of stars. Modifying the APTs could cost as much as $7,000 each. Despite these disadvantages, the best daytime technique appears to be modified daytime photometry.

IV. Estimated Capabilities of Daytime Photometry

Some daytime measurements have been made using manual location techniques on an amateur mount. Conditions present during the measurements were as follows:

(1) Date: September 17, 1988

(2) Time: 9:30 a.m. PST

(3) Location: Chilao, Angeles National Forest

(4) Elevation: approximately 6000 ft

(5) Weather conditions: hazy skies

(6) Telescope: 10-inch Meade Cassegrain

(7) Detector: Optec SSP-3 Solid State Photometer

(8) Filter: MB (centers at 754 nm, 10-nm bandwidth)

The star 19 β Orion (HD 34085) was monitored at an approximate zenith angle of 60 deg. The photometer measured 2800 counts/sec with the star in the field of view and 1400 counts/sec for the sky near the star. The starlight can thus be calculated as 1400 counts/sec. This reading yielded a signal-to-noise ratio of two. To make searching and centering of stars accurate, a signal-to-noise ratio of ten or greater is desirable. It is useful to calculate what is expected from a star of comparable magnitude in the MI band. Using this observation as a simple performance baseline for the APTs, some broad assumptions can be made. In the MB band used in the above observation, β Orion is 0.6 magnitude. The solar irradiance, which comprises most of the daytime background noise, is approximately 9000 $Wm^{-2}\mu m^{-1}$ in the MB band. If the measurements were made in the MI band, the solar irradiance would be 5500 $Wm^{-2}\mu m^{-1}$. The solar irradiance of the MI band is 0.6 times that of the MB band (see Fig. 1). The atmospheric transmission would improve from approximately 43 percent to 57 percent (see Fig. 2). This will increase the light from the star 1.33 times. From this one can see that when using the APT at 1025 nm, the signal-to-noise ratio is roughly equal to

$$\frac{1.33 \times Starlight + 0.6 \times Background\ light}{0.6 \times Background\ light} =$$

$$\frac{1.33 \times (1400) + 0.6 \times (1400)}{0.6 \times (1400)} = 3.2$$

A star 3.1 times brighter than the above example (or –0.5 magnitude in the MI band) has a signal to noise ratio of ten. There are thirteen stars brighter than –0.5 magnitude at 1025 nm (see Table 1). By allowing the telescope to view down to a zenith angle of 60 deg, eight hours of right ascension can be viewed. Any given eight hours of right ascension will provide a minimum of three, a maximum of seven, and an average of four-and-a-half observable stars brighter than –0.5 at 1025 nm (MI band). If the field of view is decreased by using a smaller, 0.5-mm diaphragm or a 2X Barlow lens, one can see stars as dim as first magnitude. There are 61 stars brighter than first magnitude at 1025 nm. With both a smaller diaphragm and a

2X Barlow lens, stars of the second magnitude would be obtainable. There are 105 stars that are brighter than second magnitude at 1025 nm.

A search has been conducted of possible daytime stars brighter than second magnitude between 1000 nm and 1200 nm [8, 9, 10]. Table 1 lists those stars visible from the southwestern United States (at least 20 deg above the horizon from a latitude of 34 deg). Figure 3 shows how these stars are distributed across the heavens. Many of the brightest of these stars are late-type stars. The blackbody curves of these older stars peak in the red and infrared. Quite a few of these late-type stars are variables [10]. The project will be able to accommodate variables with long periods or small variations (less than 0.2 magnitude). Stars with long periods will have predictable small daily variations. Small variations will not be significant in measurements. Less than seven percent of the stars listed in Table 1 are variables that cannot be used [10].

With minor equipment modifications to the APTs, daytime stellar photometry in the near infrared can produce daytime cloud cover and atmospheric transmission information.

V. Conclusions

Only one of the evaluated techniques, the modified photometry technique, is able to meet all the monitoring criteria. The degree of optimization will determine the quantity of stars the system can acquire during the day and thus how finely the sky will be monitored.

By simply using an MI filter, this technique can produce limited daytime atmospheric information. By using a single photometer and modifying it with a smaller diaphragm and/or a Barlow lens, the daytime performance will be improved. However, there will be a decrease in the number of stars obtained at night since the search routine will take longer to cover the same area. How the various daytime photometry techniques affect the project can be evaluated after the APTs are tested. The first of the APTs should have been delivered about March 1989.

By using an instrument selector and a second photometer, the systems can be modified to increase the number of stars that are seen in the day without changing the performance at night. With this minor equipment change, daytime stellar photometry can provide atmospheric transmission data derived from an average of 30 evenly distributed stars at any given time.

Acknowledgment

References

[1] *Geophysical Instruments and Systems Catalog 1987*, Qualimetrics Inc., Sacramento, California, pp. 27–28, 192–193, 1987.

[2] K. McGuffie, A. Henderson-Sellers, "Observations of Oceanic Cloudiness," *EOS Transactions*, American Geophysical Union, vol. 69, no. 28, pp. 714–715, July 1988.

[3] R. W. Johnson, W. S. Herin, "Automated Cloud Cover Measurements with a Solid-State Imaging System," In House Technical Note No. 206, University of California, San Diego, Scripps Institution of Oceanography, Visibility Laboratory, La Jolla, California, July 1987.

[4] A. W. F. Cousins, "VRI Standards in the E Regions," *Memoirs of the Royal Astronomical Society*, vol. 81, pp. 25–36, 1976.

[5] *Model SSP-3 Solid-State Stellar Photometer, Technical Manual*, Optic Inc., Lowell, Michigan, October 1988.

[6] P. R. Gast, "Solar Irradiance," in *Handbook of Geophysics and Space Environments*, Section 16.1, Cambridge, Massachusetts: S. L. Valley, 1965.

[7] D. E. Novoseller, "Use of Lowtran in E Transmission Calculations," *Applied Optics*, vol. 26, pp. 3185–3186, 1987.

[8] G. Neugebauer, R. B. Leighton, "Two-Micron Sky Survey, A Preliminary Catalog," National Aeronautics and Space Administration Special Publication SP-3047, Washington D.C., 1969.

[9] D. Y. Gezari, M. Schmitz, J. M. Mead, *Catalog of Infrared Observations*, 1st ed., National Aeronautics and Space Administration Reference Publication RP-1118, Washington D.C., 1984.

[10] D. Hoffleit, C. Jaschek, *The Bright Sky Catalogue*, 4th ed., Yale University Observatory, New Haven, Connecticut, 1982.

Table 1. Stars brighter than second magnitude (1000 nm to 1200 nm)

Henry Draper (HD) no.	Right Ascension	Declination	Magnitude	Type
432	00 07 47.5	+59 08 59	1.65	F2III-IV
1760	00 21 46.3	−20 03 28	1.02	M5IIe
3627	00 39 19.6	+30 51 40	1.24	K3III
3712	00 40 30.4	+56 32 15	0.42	KOIIIa
4128	00 43 35.3	−17 59 12	0.39	KOIII
6860	01 09 43.8	+35 37 14	−0.25	MOIIIa
12533	02 03 53.9	+42 19 47	0.26	K3-IIb
12929	02 07 10.3	+23 27 45	0.28	K2IIIab
14386	02 19 20.7	−02 58 39	−1.70	M7IIIa
17506	02 50 41.8	+55 53 44	1.05	M3Ib-IIa
18884	03 01 40.6	+04 05 23	−0.29	M1.5IIIa
18925	03 03 47.7	+53 30 23	1.70	G8III+A2V
19058	03 05 10.5	+38 50 25	−0.10	M4II
20720	03 19 30.9	−21 45 28	0.00	M2III
20902	03 24 19.3	+49 51 41	0.87	F5Ib
23475	03 49 31.2	+65 31 34	0.51	M2IIab
25025	03 58 01.7	−13 30 31	0.35	M0.5III
29139	04 35 55.2	+16 30 33	−1.16	K5III
29755	04 40 26.4	−19 40 18	0.69	M4III
31398	04 56 59.6	+33 09 58	−0.74	K3II
32068	05 02 28.6	+41 04 33	1.10	K4IIB8V
32887	05 05 27.6	−22 22 16	1.48	K5IIIV
33664	05 11 22.8	−11 50 57	−0.10	M6III
34085	05 14 32.2	−08 12 06	1.15	B8Iae
34029	05 16 41.3	+45 59 53	−1.17	G5IIIe
35497	05 26 17.5	+58 36 27	1.96	B7III
36079	05 28 14.7	−20 45 34	−1.33	G5II
36389	05 32 12.7	+18 35 39	0.82	M2Iab-Ib
37128	05 36 12.7	−01 12 07	2.00	BOIae
39801	05 55 10.3	+07 24 25	−2.68	M2Ia-Iab
40183	05 59 31.7	+44 56 51	1.85	A2IV
40239	05 59 56.1	+45 56 13	0.30	M3III
42995	06 14 52.6	+22 30 24	−0.23	M3III
44478	06 22 57.6	+22 30 49	−0.28	M3IIIab
47105	06 37 42.7	+16 23 57	1.91	AOIV
48329	06 43 55.9	+25 07 52	0.99	G8Ib
48915	06 45 08.9	−16 42 58	−1.33	AIVm
52089	06 58 37.5	−28 58 20	1.97	B2II
52877	07 01 43.1	−27 56 06	0.93	K7Ib
54605	07 08 23.4	−26 23 35	0.07	F8Ia
60179	07 34 35.9	+31 53 18	1.55	AIV
61421	07 39 18.1	+05 13 30	−0.41	F5IV-V
62509	07 45 18.9	+28 01 34	−0.35	KOIIIb
69267	08 16 30.9	+09 11 08	1.09	K4III
76294	08 55 23.6	+05 56 44	1.48	G9-II-III
80493	09 21 03.2	+34 23 33	0.65	K7IIIab
81797	09 27 35.2	−08 39 31	−0.36	K3II-III
84748	09 47 33.4	+11 25 43	−0.40	M8IIIe
87901	10 08 22.3	+11 58 02	1.47	B7V
89484	10 19 58.3	+19 50 30	−0.67	KI-IIIb
89758	10 22 19.7	+41 29 58	0.60	MOIII
93813	10 49 37.4	−16 11 37	1.06	K2III
95689	11 03 43.6	+61 45 03	0.05	KOIIIa
100029	11 31 24.2	+64 19 52	1.62	MOIII
102647	11 49 03.5	+14 34 19	1.99	A3V
105707	12 10 07.4	−22 37 11	1.61	K2.5IIIa
109379	12 34 23.2	−23 23 48	1.23	G5II

Table 1 (contd)

| Henry Draper (HD) no.	Right Ascension	Declination	Magnitude	Type
112300	12 55 36.1	+03 23 51	0.08	M3III
113226	13 02 10.5	+10 57 33	1.52	G8IIIab
116658	13 25 11.5	−11 09 41	1.50	B1III-IV
120315	13 47 32.3	+49 18 48	−0.19	B3V
120285	13 49 02.0	−28 22 03	−1.12	M7.5-M9pe
121370	13 54 41.0	+18 23 51	1.65	GOIV
124897	14 15 39.6	+19 10 57	−1.95	KIIIb
127665	14 31 20.1	+30 22 17	1.46	K3III
129988	14 44 29.1	+27 04 27	0.65	KOII-III
131873	14 50 42.2	+79 09 19	1.47	K4III
132813	14 57 34.8	+65 55 56	0.73	M5III
133216	15 04 04.1	−25 16 55	0.02	M3IIIa
140573	15 44 16.0	+06 25 32	1.99	K2 III
146051	16 14 20.6	−03 41 39	0.54	M0.5III
148387	16 23 59.3	+61 30 51	1.17	G8IIIab
148478	16 29 24.3	−26 25 55	−2.69	M1.5Iab-Ib
148783	16 28 38.4	+41 52 54	−0.20	M6III
148856	16 30 13.1	+21 29 22	1.21	G7IIIa
150680	16 41 17.1	+31 36 10	1.70	GOIV
156014	17 14 38.8	+14 23 25	−2.11	M5Ib-II
156283	17 15 0.26	+36 48 33	0.80	K3IIab
159181	17 30 25.8	+52 18 05	1.29	G2Ib-IIa
159561	17 34 55.9	+12 33 36	1.71	A5III
164058	17 56 36.2	+51 29 20	−0.39	K5III
168454	18 20 59.5	−29 49 42	1.20	K3IIIa
169916	18 27 58.1	−25 25 18	1.72	KIIIb
172167	18 36 56.2	+38 47 01	−0.02	A0Va
175865	18 55 19.9	+43 56 46	−0.32	M5III
180711	19 12 33.1	+67 39 41	1.43	G9III
183912	19 30 43.1	+27 57 35	+1.13	K3II
186791	19 46 15.4	+10 36 48	0.24	K3II
187076	19 47 23.0	+18 32 03	0.37	M2II+AOV
187642	19 50 46.8	+08 52 06	0.39	A7V
189319	19 58 45.3	+19 29 32	1.79	MOIII
192909	20 15 28.1	+47 42 51	1.19	K3Ib+B3V
194093	20 22 13.5	+40 15 24	1.22	F8Ib
197345	20 41 25.8	+45 16 49	0.91	A2Iae
197989	20 46 12.5	+33 58 13	0.91	KOIII
200905	21 04 55.7	+43 55 40	1.26	K4-5Ib-II
204867	21 31 33.3	−05 34 16	1.61	GOIb
205730	21 36 02.2	+45 22 29	−1.41	M5IIae
210745	22 10 51.1	+58 12 05	0.97	K1.5b
213310	22 29 31.7	+47 42 25	1.65	MOII+B8V
216386	22 52 36.6	−07 34 47	0.92	M2.5IIIa
216956	22 57 38.9	−29 37 20	1.99	A3V
217906	23 03 46.3	+28 04 58	−0.64	MK2.5II-III
224935	00 01 57.5	−06 00 51	1.44	M3III
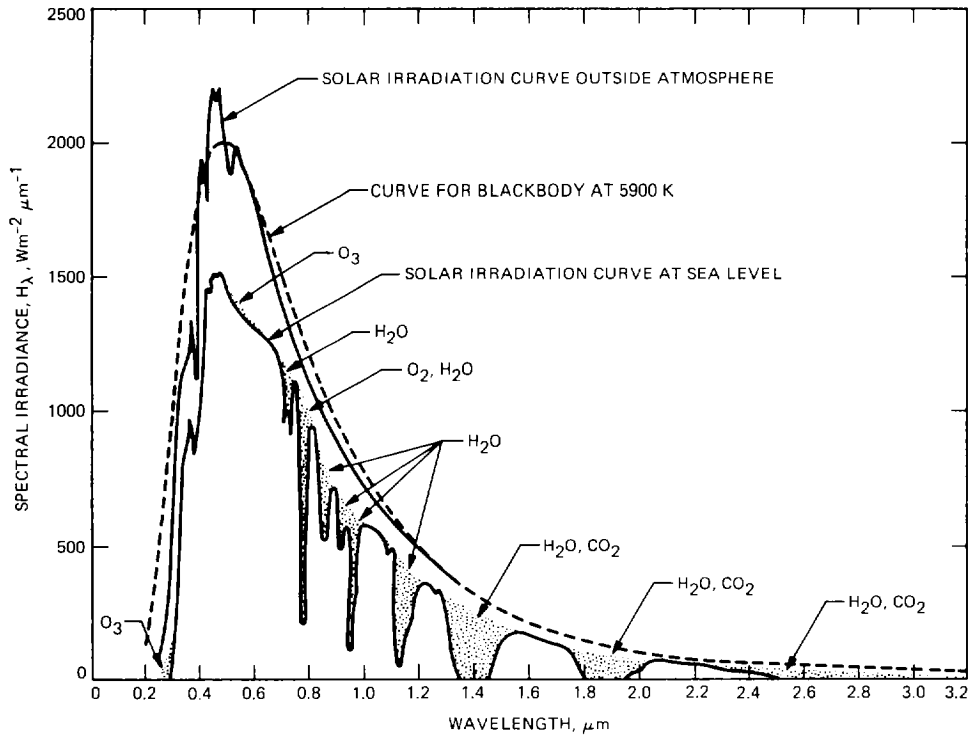
Fig. 1. Solar spectral irradiance with the sun at zenith. Absorption bands are shown shaded [6].
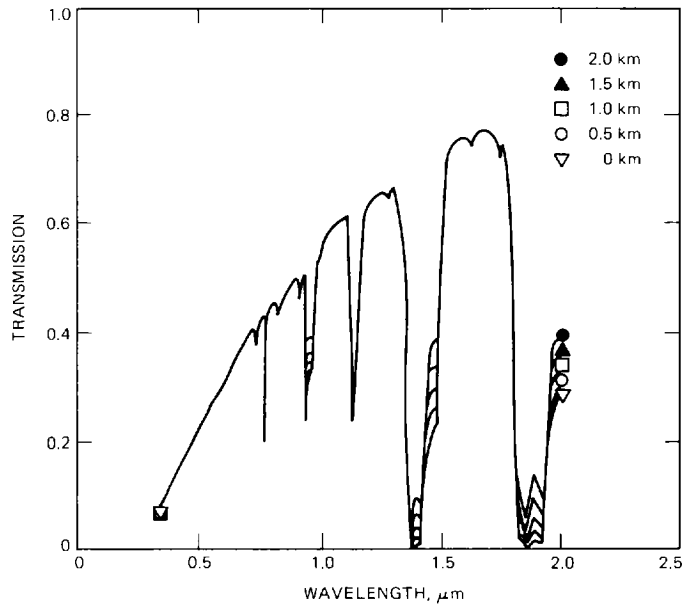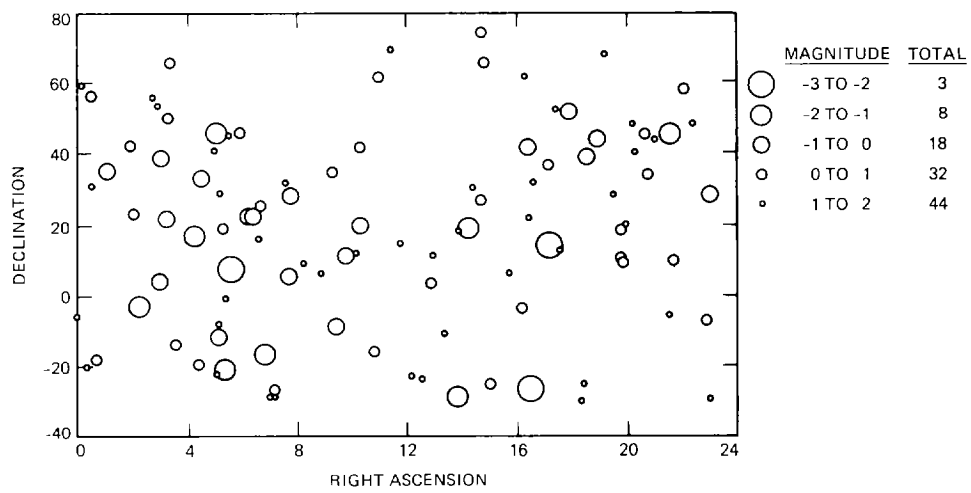

Fig. 2. LOWTRAN6 calculation of space-to-ground transmission as a function of wavelength in the presence of mid-latitude winter haze. The curves correspond to transmitter altitude [7].

MAGNITUDE TOTAL

-3 TO -2   3
-2 TO -1   8
-1 TO 0   18
0 TO 1   32
1 TO 2   44

80

60

40

DECLINATION

20

0

-20

-40

0   4   8   12   16   20   24

RIGHT ASCENSION

Fig. 3. Stars brighter than second magnitude at 1025 nm.